

# Equilibrium Disperse Dye Sorption by Drawn Polypropylene Films

KOICHIRO YONETAKE, KOTOKU NAGAMATSUYA, and TORU MASUKO, *Faculty of Engineering, Yamagata University, Jonan-4, Yonezawa-shi, Yamagata-ken, 992 Japan*

## Synopsis

Isotactic polypropylene (PP) films drawn at various temperatures ranging from 100 to 155°C have been dyed at 80°C with p-aminoazobenzene (PAAB) or C.I. Disperse Yellow 7 (Y-7). The equilibrium dye sorption ( $M_0$ ) of PAAB obtained for these films decreased with an increase in draw ratio ( $\lambda$ ) of the films. The  $M_0$  values of Y-7, however, increased with increasing  $\lambda$ ; similarly the crystallinities of these films increased slightly with draw ratios. By use of fine structural data of these films, the change in  $M_0$  of Y-7 for drawn PP films were analyzed in terms of a mosaic-block structural model. The increase in  $M_0$  with increasing  $\lambda$  was thus ascribed to enhanced sorption by the amorphous side region between crystalline cores located parallelly in the direction to the molecular axis. The side regions of the drawn systems become rich in interfibrillar tie chains in a higher range of  $\lambda$ . The side region seem to have a strong affinity particularly to a long rodlike dye molecule such as Y-7; this feature is probably associated with the amount of the amorphous chains having extended chain conformation, the fraction of which increases during drawing.

## INTRODUCTION

It has been communicated by Morizane et al.<sup>1</sup> that the equilibrium sorption of C.I. Acid Orange 10 in drawn nylon 6 monofilaments is larger than that in undrawn filaments. Sumida et al.<sup>2</sup> have also reported that the equilibrium uptakes of the Whitex SNK by high density polyethylene (HDPE) films increase monotonically with an increase in draw ratio ( $\lambda$ ) of HDPE, suggesting that this result is attributable to an increase in free energy of amorphous regions accompanied by molecular orientation or an increase in microvoids during a drawing process. Similarly, it has observed that the equilibrium uptakes ( $M_0$ ) of C.I. Disperse Yellow 7 (Y-7) by drawn polypropylene (PP) films increase with a rise in their orientation.<sup>3</sup>

In general, when a polyolefin film is highly drawn, the equatorial scattering emerges on the small angle X-ray scattering (SAXS) patterns, which is the evidence of long and narrow longitudinal voids in the specimen.<sup>4</sup> However, it seems to be difficult to obtain a well-defined relationship between the void content and the amount of equilibrium dye sorption.

On the relationship between dyeability and unoriented polymer structures, we have proposed a new dyeing model on the basis of the mosaic block structural model of polymeric materials (HDPE and PP).<sup>5,6</sup> In this dyeing model, the amorphous region of a semicrystalline polymer has been divided into two separate regions. One is the amorphous end region composed of fold, cilia, and tie chains, and the other is the amorphous side region composed of extended amorphous chains originated from crystallo-

graphic misfits in lattice chains. The  $M_0$  values can be divided into respective sorptions by the side and end regions in terms of this dyeing model. The dye uptake of the side region increases with an increase in crystallinity. In particular, long rodlike dye molecules, such as Y-7, prefer to bind much more tightly to the chains with extended chain conformations. This dyeing model has also been applicable to the system of Y-7 and PP films treated with various organic solvents.<sup>7</sup>

The purpose of the present study is to test whether or not the proposed mosaic block dyeing model is available to the dyeing behavior of PP films drawn at various temperatures.

## EXPERIMENTAL

### Materials

The PP film of commercial type with its weight-average molecular weight  $\overline{M}_w = 2.62 \times 10^5$  ( $\overline{M}_w/\overline{M}_n = 4.2$ ) and 96% tacticity (a residue of extraction with boiling *n*-heptane) was hot-pressed into a film of 200  $\mu\text{m}$  thick at 230°C and  $4.9 \times 10^6$  Pa (50 kg/cm<sup>2</sup>) for 10 min, followed by quenching into ice water.

### Drawing

A quenched film was mounted to a manual stretching device, and it was drawn in polyethylene glycol (PEG) at desired temperatures ( $T_d$ ) ranged from 100 to 155°C, after preheated at  $T_d$  for 10 min. The draw ratios  $\lambda$  ranged from 1.0 to 12. The rate of drawing was 1 cm/min. After drawing, the film was immediately quenched into ice water, and then it was washed with running water for a day. No necking was observed in each drawing process.

### Dyeing

Disperse dyes used are purified *p*-aminoazobenzene (PAAB) and C.I. Disperse Yellow 7. Some of their characteristics are already shown in the previous paper.<sup>6</sup> Each dye bath was prepared by dissolving the dye (Y-7: 40 mg, PAAB: 250 mg) in 2500 mL of deionized water at 80°C with 1 g of a nonionic surfactant, Neugen HC (Daiichi Kogyo Seiyaku Co.). Drawn PP films were dyed at 80°C for 240 h to equilibrium dye uptake. The dye sorbed by the film was extracted with chlorobenzene at 70°C and its amount in the solvent was measured spectrophotometrically using a Hitachi 124 spectrophotometer.

### Structural Characterization

All the samples structurally examined were dyed ones. The determination of density ( $\rho$ ) was made on a density gradient column consisting of water and 1-propanol at 25°C.

X-ray measurements were carried out on a Rota Flex RU-3 (Rigaku Denki Co.) using Ni-filtered Cu-K $\alpha$  radiation generated at 40 kV and 100 mA. The

values of crystalline weight fractions ( $C_x$ ) of the samples were determined by the Weidinger-Hermans method.<sup>8</sup> The values of volume crystallinity ( $C_v$ ) were approximated by  $C_v = (\rho/\rho_c)C_x$ , where  $\rho_c = 0.9354 \text{ g/cm}^3$ .<sup>9</sup> The crystalline size normal to ( $hkl$ ) planes ( $l_{hkl}$ ) was estimated by Scherrer's equation<sup>10</sup> (the constant  $K = 1.0$ ) from the integral width of wide-angle X-ray diffraction (WAXD) traces. When the intensity of a WAXD trace for each drawn film was measured, the sample was rotated at 1000 rpm in order to avoid problems which arise from orientation effects. Long period ( $L_p$ ) was determined photographically by use of a pinhole small-angle X-ray scattering (SAXS) camera. The dichroic orientation factor ( $f_D$ ) of a PP film dyed with Y-7 was calculated by the next equation<sup>11</sup>

$$f_D = (K_{\parallel} - K_{\perp}) / (K_{\parallel} + 2K_{\perp}) \cdot D_0 \quad (1)$$

where  $K_{\parallel}$  and  $K_{\perp}$ , respectively, are absorbances for polarized light vibrating parallelly and perpendicularly to the draw direction of the film.  $D_0$  is the intrinsic dichroism ( $D_0 = 1$ ) of Y-7.<sup>11</sup> The absorbances of  $K_{\parallel}$  and  $K_{\perp}$  were measured at room temperature by use of a Shimadzu Aqv-50 Spectrophotometer with a polarizer.<sup>12</sup>

## RESULTS AND DISCUSSIONS

### Fine Structural Changes in Polypropylene Films during Drawing Procedures

The changes in  $L_p$  are plotted as a function of  $\lambda$  in Figure 1, where  $L_p$  increases with an increase in  $\lambda$  in each case. These features are similar to those obtained by Samuels<sup>13</sup> and Baltá-Calleja and Peterlin.<sup>14</sup> However, the  $L_p$  values obtained in the present study are slightly larger than those observed in above workers' investigations over the whole draw ratios. Such differences in  $L_p$  probably come from the different heating medium em-

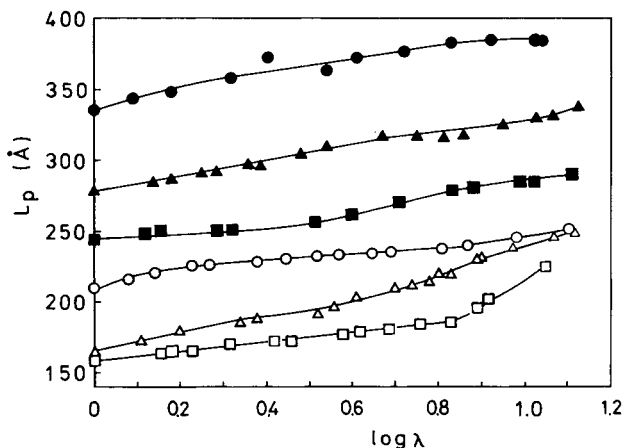


Fig. 1. Changes in long period as functions of draw ratios: (●), (▲), (■), (○), (△), and (□) for the samples drawn at 155, 150, 145, 140, 120, and 100°C, respectively.

ployed in drawing experiments; a PEG bath was used in the present study and they used an air oven.

The changes of  $C_v$  are illustrated against  $\lambda$  in Figure 2. The values of  $C_v$  increase with an increase in  $T_d$  over the whole range of  $\lambda$ . The  $C_v$  values of undrawn samples depend on annealing or preheating temperatures ( $= T_d$ ), because original undrawn films are preheated at  $T_d$  for 10 min just before drawing. A secondary crystallization occurs in this procedure. The  $C_v$  values of samples drawn below 145°C increase with increasing  $\lambda$ . On the other hand, those of samples drawn above 150°C remain almost unchanged.

The changes in  $L_p$  are plotted as a function of  $C_v$  in Figure 3. The values of  $L_p$  increase with increasing  $C_v$  up to  $C_v = 0.55$ . Interestingly, the relation between  $L_p$  and  $C_v$  can be indicated by one curve in this range. This feature suggests that the increase in  $C_v$  is ascribable to the thickening of crystalline lamellae. The  $C_v$  values of samples drawn above 150°C, however, remain almost unchanged in spite of the increase in  $L_p$  with increasing  $\lambda$  and  $T_d$ . To interpret this feature, we consider the reason as follows: recrystallization during drawing increase the amount of crystal region; at the same time, the amount of amorphous region also increases by partial melting of thermodynamically unstable crystallites and by broadened interlamellar spacing during drawing. If the rate of recrystallization is balanced with those of partial melting and broadened interlamellar spacing, the  $C_v$  values possibly remain almost unchanged during drawing.

The changes in  $l_s$ , the crystallite width perpendicular to the molecular axis, are plotted against  $\lambda$  in Figure 4. The values of  $l_s$  were approximated by the equation  $l_s = (l_{040} \cdot l_{110})^{1/2}$ . In the initial stages of drawing processes, the values of  $l_s$  keep themselves in almost constant but different values corresponding to drawing temperatures; at  $\lambda = 3$ , they start to decrease gradually and converge to the value of ca. 110 Å at higher draw ratios. Presumably this feature is a reflection that microspherulitic structures in the PP film are destroyed by drawing, and they slowly transform into microfibrillar structures. The width of 110 Å corresponds to those of microfibrils formed in the film. On the other hand, in the samples drawn

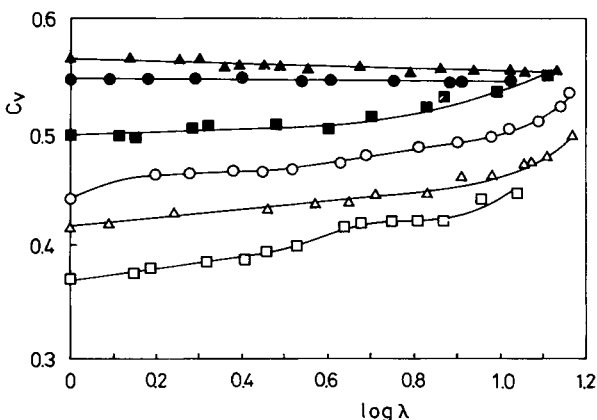


Fig. 2. Changes in volume crystallinity as functions of draw ratios. The marks are the same as those utilized in Figure 1.

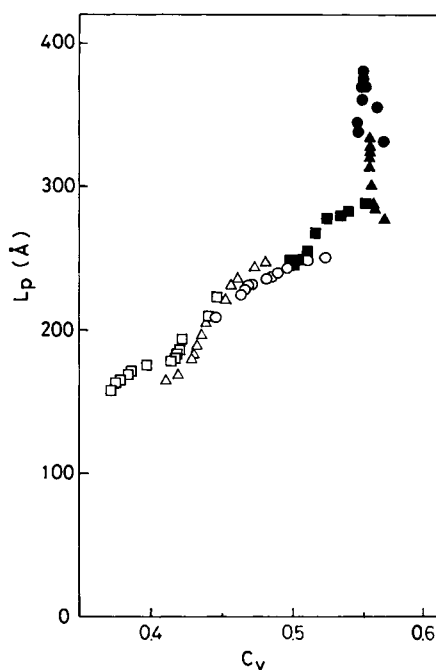


Fig. 3. Changes in long period as functions of volume crystallinity. The marks are the same as those utilized in Figure 1.

above  $150^{\circ}\text{C}$ , the decrease in  $l_s$  begins at  $\lambda = 5$ . The tensile stress within the above samples during drawing is less than that of samples drawn at lower temperatures because amorphous chains in the samples drawn at higher temperatures are much more relaxed. Therefore, the plastic deformation of spherulites occurs at relatively higher draw ratios in the samples drawn above  $150^{\circ}\text{C}$ .

During above deformation process, amorphous chains become oriented in the direction of applied stress. Figure 5 shows the changes in  $f_D$  against  $\lambda$ .

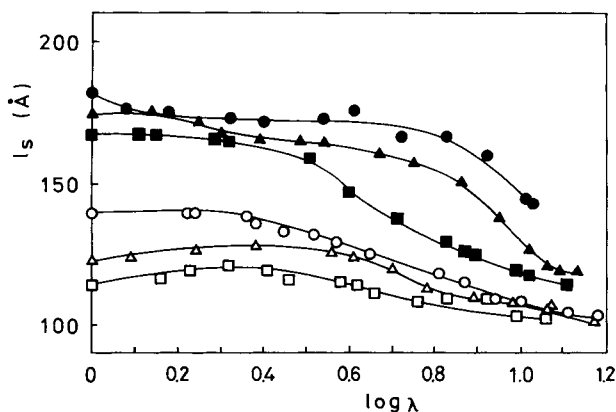


Fig. 4. Changes in crystalline size ( $l_s$ ) as functions of draw ratios. The marks are the same as those utilized in Figure 1.

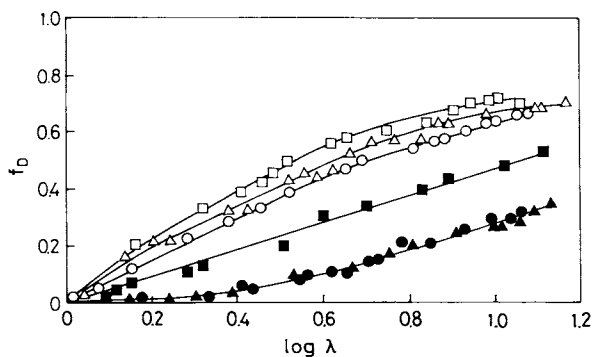


Fig. 5. Changes in dichroic orientation factor as functions of draw ratios. The marks are the same as those utilized in Figure 1.

The  $f_D$  values increase monotonically with increasing  $\lambda$ , and also they decrease with an increase in  $T_d$ . At higher temperatures of  $T_d$ , the amorphous chains cannot sufficiently be oriented during drawing, since the segmental mobilities in PP films increase.

The findings above suggest that the structural deformation process of the samples drawn above  $150^\circ\text{C}$  is somewhat different from that of the samples drawn below  $145^\circ\text{C}$ . The difference in fine structures between the samples of above two processes will be further discussed in a later section.

### Dye Sorption

The equilibrium uptakes  $M_0$  of PAAB obtained are plotted against  $\lambda$  in Figure 6. The values of  $M_0$  decrease monotonically with an increase in  $\lambda$  except the samples drawn at  $150^\circ\text{C}$ . These values are plotted against  $C_v$  in Figure 7, where  $M_0$  decreases with increasing in  $C_v$  in each case. The reduction of  $M_0$  is induced by the decrease in the amount of the amorphous region in which PAAB molecules can dissolve. These results can simply be interpreted in terms of the two phase model of polymer materials. The  $M_0$  values of Y-7, on the other hand, increase with a rise in  $\lambda$  in every case,

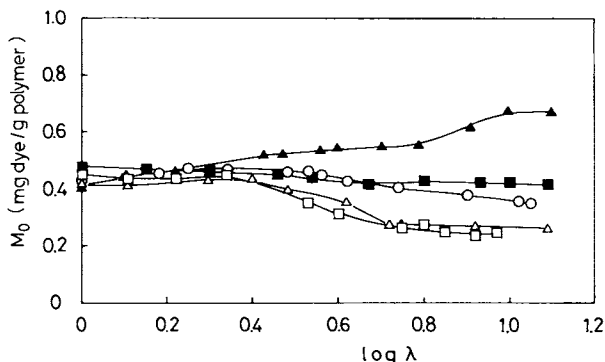


Fig. 6. Variations of equilibrium dye uptakes of PAAB vs. draw ratios. The marks are the same as those utilized in Figure 1.

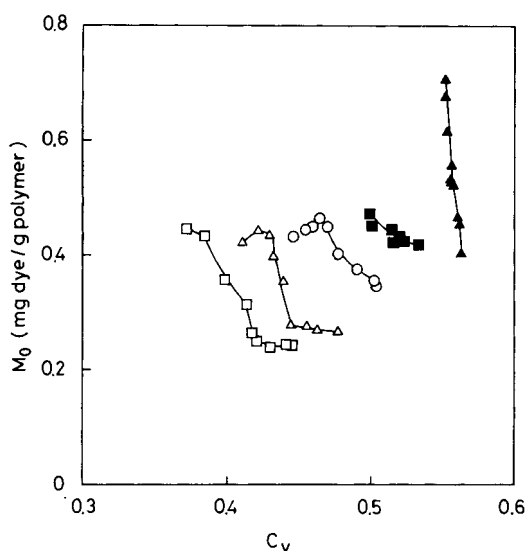


Fig. 7. Variations of equilibrium dye uptakes of PAAB vs. volume crystallinity. The marks are the same as those utilized in Figure 1.

as shown in Figure 8, and they increase with increasing  $C_v$  (Fig. 9). These findings cannot be interpreted from the viewpoint of the two phase model. Above feature is similar to the trends obtained for drawn HDPE films dyed with Whitex SNK.<sup>2</sup> As described earlier, Sumida et al.<sup>2</sup> have proposed that the increase in the equilibrium uptakes of Whitex SNK is associated with the increase in microvoids formed in PE film during drawing. In the present study, however, the values of  $M_0$  of PAAB decrease with increasing  $\lambda$  (Fig. 6). If dye molecules are absorbed by microvoids,  $M_0$  of PAAB as well as Y-7 should increase with increasing  $\lambda$ . Consequently, it is difficult to interpret above findings from the concept of microvoid contents systematically.

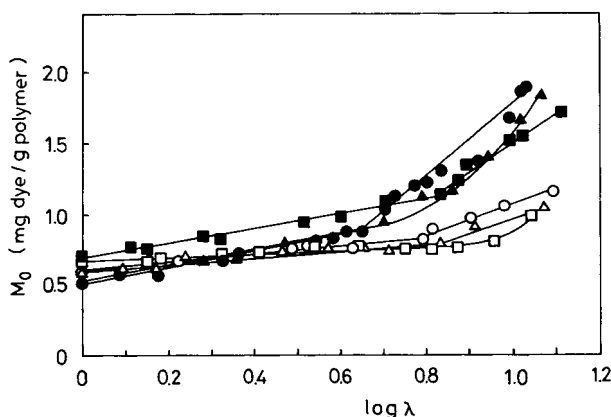


Fig. 8. Variation of equilibrium dye uptakes of Y-7 vs. draw ratios. The marks are the same as those utilized in Figure 1.

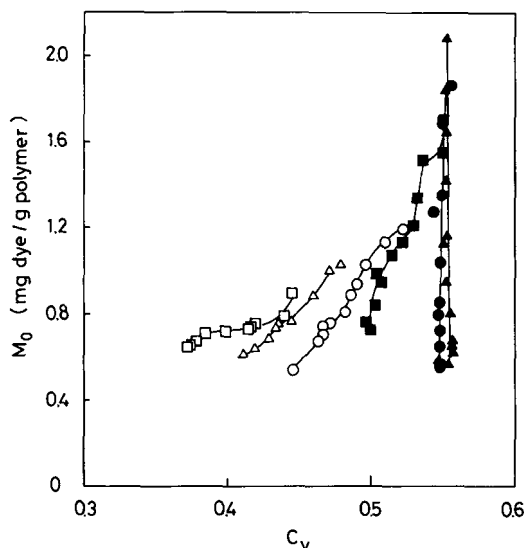


Fig. 9. Variations of equilibrium dye uptakes of Y-7 vs. volume crystallinity. The marks are the same as those utilized in Figure 1.

## Dye Sorption Interpreted by the Mosaic Block Dyeing Model

### *Mosaic Block Dyeing Model*

In the deformation process of a polyolefin film, lamellar crystallites located in the original spherulitic film break down to smaller crystallites and occasionally parts of them transform to amorphous regions.<sup>13</sup> Sometimes amorphous chains in a drawn film recrystallize to various thicknesses of crystallites depending upon drawing temperatures. Finally microspherulitic structures are destroyed and gradually microfibrillar structures containing lamellar crystallites are formed in the oriented film.<sup>15</sup> Therefore, we can consider anytime lamellar crystallites as the units of fine structures in variously drawn systems.

Lamellar crystallites are supposed to be composed of small mosaic blocks.<sup>16</sup> Figure 10 illustrates a schematic representation of the mosaic block model in a microfibril structure. According to the mosaic block dyeing model,<sup>5</sup> the equilibrium dye uptake/g polymer,  $M_0$ , can be divided into the dye uptakes in the amorphous side region ( $M_s$ ) and the end region ( $M_e$ ), as in the following expression;

$$M_0 \cdot \rho = (K_s \cdot V_s/V_b + K_e \cdot V_e/V_b) \cdot c \quad (2)$$

$$M_0 = M_s + M_e \quad (3)$$

where  $V_b$  is volume of a mosaic block and  $V_s$  and  $V_e$  are the respective volumes of the amorphous side region and the end region. The coefficient  $K_s$  for the spherulitic films has been assumed as  $K_s = l_c \cdot m_s$ , where  $l_c$  is the stem length and  $m_s$  is the constant independent of both the fine structural parameters and the dye bath concentration. In the undrawn samples,<sup>5,6</sup> we



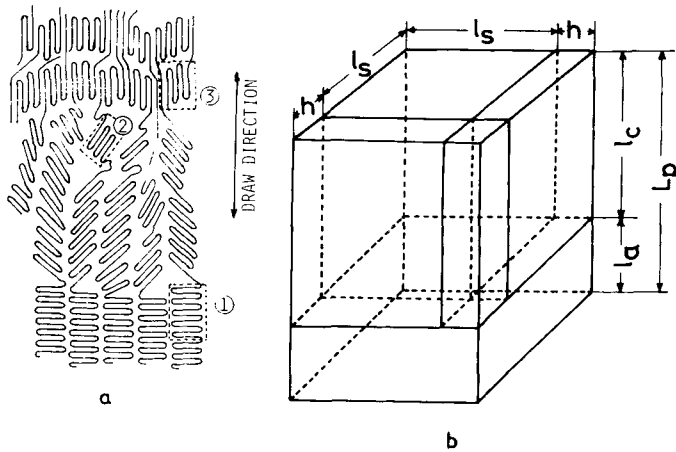


Fig. 10. Schematic representation of a mosaic block in a drawn sample: (a) A model for fiber formation (Peterlin)<sup>17</sup>; ①, ②, and ③ are crystalline blocks; (b) a mosaic block model for crystalline blocks; ①, ②, and ③, shown in Figure 1(a).

have considered that the equilibrium sorption by the side region is proportional to the  $l_c$  as a measure of the channel length through which dye molecules can diffuse. In drawn samples, microfibril structures are formed in the higher range of  $\lambda$ , and the interfibrillar region (side region) is rich in the extended tie chains. Therefore, it is necessary to consider the effect of drawing on the dyeability of the side region in drawn samples. We modify intuitively the coefficient  $K_s$  as in the following expression;

$$K_s = \lambda \cdot l_c \cdot m_s \tag{4}$$

where  $\lambda$  is draw ratio. This expression includes an isotropic case of  $\lambda = 1$ . Alternatively,  $K_e$  is assumed to be constant, since the dyeability of the end region consisting of chain folds will not change so much even in a drawing process. We express  $M_s$  and  $M_e$  in terms of fine structural parameters by the next equation<sup>5</sup>:

$$M_s = K_s \cdot V_s \cdot c / V_b \cdot \rho \tag{5}$$

$$= \lambda \cdot m_s \cdot C_v^2 L_p (2 + p) p (1 + p)^2 c / \rho \tag{6}$$

$$M_e = K_e \cdot V_e \cdot c / V_b \cdot \rho$$

$$= K_e [1 - (1 + p)^2 C_v] \cdot c / \rho$$

where  $p = h/l_s$ . Substitution of eqs. (5) and (6) into (2) yields the next expression:

$$M_0 = C_v^2 \cdot (2 + p) p (1 + p)^2 L_p \cdot \lambda \cdot m_s \cdot c + [1 - (1 + p)^2 C_v] K_e \cdot c \tag{7}$$

Equation (7) can be expressed by

$$\eta = \lambda \cdot \xi \cdot m_s \cdot c + K_e \cdot c \tag{8}$$

where

$$\eta = M_0 \cdot \rho / [1 - (1 + p)^2 C_v] \quad (9)$$

$$\xi = C_v^2 (2 + p) p (1 + p)^2 L_p / [1 - (1 + p)^2 C_v] \quad (10)$$

If a linear relationship holds between the measurable quantities of  $\lambda \cdot \xi$  and those of  $\eta$ ,  $m_s c$ , and  $K_e c$  can be determined from the slope and the intercept of this relationship, respectively. Using both constants determined above, we can estimate the quantities of  $M_s$  and  $M_e$ . The linear relationship between  $\lambda \cdot \xi$  and  $\eta$  [eq. (8)] may approve that the structural change with drawing has an effect on the increasing  $K_s$ . Through the above procedure, we can discuss the partition characteristics of disperse dyes into the side and end regions in drawn PP samples.

#### *Dye Sorption by the Side and End Regions*

By use of the structural parameters shown in the previous section, the test plot of  $\eta$  vs.  $\lambda \cdot \xi$  are displayed in Figure 11, yielding a fairly good linear relationship. The line drawn is obtained from the least-squares fits of the numerical data. The value of  $p$  is assumed to be 0.1 irrespective of various draw ratios and various drawing temperatures, when both values of  $\eta$  and  $\xi$  are calculated from eqs. (9) and (10). This value ( $P = 0.1$ ) is equal to that assumed in isotropic films.<sup>5-7</sup> The most striking feature of these results is that the relation between  $\eta$  and  $\lambda \cdot \xi$  can be indicated by just one straight line independent of various drawing temperatures. Consequently, both coefficients of dye sorption ( $K_s$  and  $K_e$ ) are independent of drawing temperatures.

We can then calculate the quantities of  $M_s$  and  $M_e$  for each sample using the values of  $m_s c$  and  $K_e c$  determined. These quantities of the samples drawn at 140 and 150°C are plotted against  $\lambda$  in Figures 12 and 13, respectively. The quantities of  $M_s$  increase remarkably with an increase in  $\lambda$ . This trend

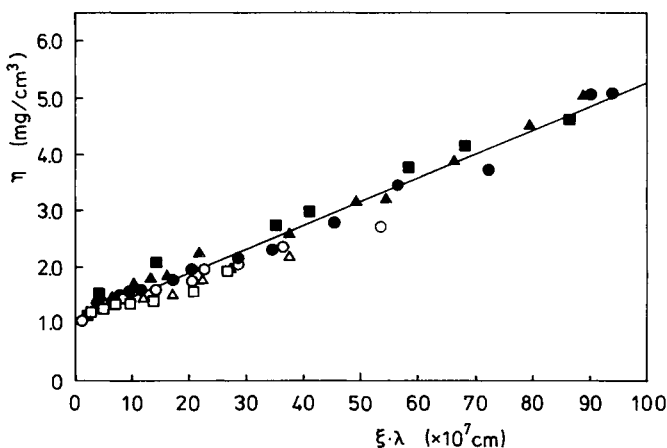


Fig. 11. Test plots based on eq. (3). The line is determined by the least squares fits for the data of Y-7. The symbols correspond to those utilized in Figure 1.

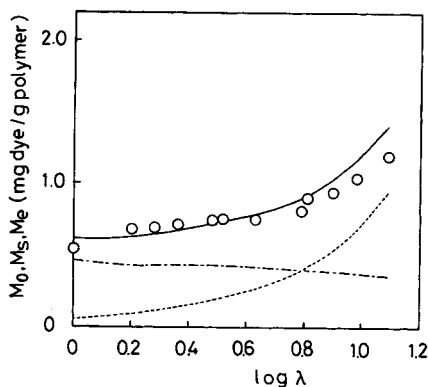


Fig. 12. Variation of the equilibrium dye uptake of Y-7 by samples drawn at 140°C vs. draw ratios. The mark of (○) indicates experimental points and the line through points is a theoretical curve of total sorption ( $M_0$ ). The dotted line (---) and broken line (---) are, respectively, the theoretical curves of sorption by the side region ( $M_s$ ) and by the end region ( $M_e$ ).

is observed in every case, though not indicated graphically. On the other hand,  $M_e$  of the samples drawn below 145°C decreases slightly with increasing  $\lambda$ ; and  $M_e$  of the samples drawn above 150°C remains almost constant in whole range of  $\lambda$ , as shown in Figures 12 and 13, respectively.

The volume fraction of the end amorphous region,  $V_e/V_b$ , is shown as a function of  $\lambda$  in Figure 14. The values of  $V_e/V_b$  of the samples drawn below 145°C decrease slightly. Thus, the change in  $M_e$  is reasonably attributable to the change in  $V_e/V_b$ , since the  $K_e$  parameter is constant in the whole range of  $\lambda$  as noted above. The values of  $V_e/V_b$  of the samples drawn above 150°C remain almost unchanged. Therefore, the dye uptakes by the end region depend on the volume fraction of the end region even in the drawn PP films.

Figure 15 shows the changes in  $V_s/V_b$  against  $\lambda$ . The values of  $V_s/V_b$  remains almost constant in the whole range of  $\lambda$  in each case in spite of

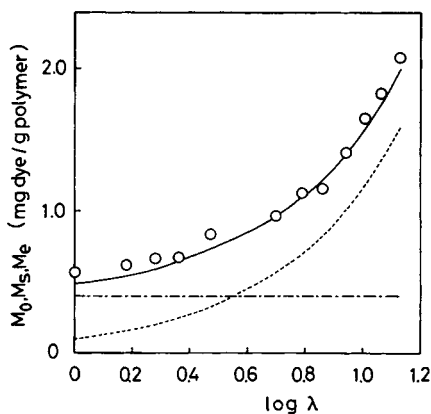


Fig. 13. Variation of the equilibrium dye uptake by samples drawn at 150°C vs. draw ratios. The marks and lines are the same as those utilized in Figure 12.

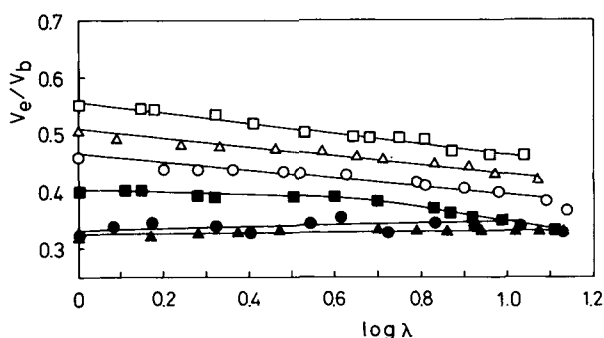


Fig. 14. Changes in the volume fraction of the end region against draw ratios. The marks are the same as those utilized in Figure 1.

the increase in  $M_s$  with increasing  $\lambda$ . The above findings suggest that the change in  $M_s$  is caused mainly by the change in  $K_s$  values.

The side region of an oriented system in the higher range of  $\lambda$  is rich in interfibrillar tie chains, having extended chain conformation. These tie chains may build up new channels in interfibrillar boundaries, through which dye molecules can penetrate. When the microfibrils become oriented along the fiber axis, the conformation of tie chains in the side region will be much more extended; thus these channels also line up along these microfibrils. In addition, the mobility of the amorphous chains in the side region decreases during drawing, since these chains become more oriented. Long rod-shaped Y-7 molecules will be able to align these chains more closely in the higher range of  $\lambda$ . So we can expect that it is much easier for Y-7 molecules to bind tightly to the amorphous chains accompanied by drawing.

Finally, Figure 16 shows schematic models which explain changes in dye sorption modes during drawing. Figures 16(a) and 16(b) illustrate models for samples drawn below 145 and above 150°C, respectively. The transformation from the spherulitic structure to the microfibrillar structure, starts at  $\lambda = 3$  in samples drawn below 145°C, and it starts at  $\lambda = 5$  in samples drawn above 150°C. Since these microfibrils are not highly oriented along

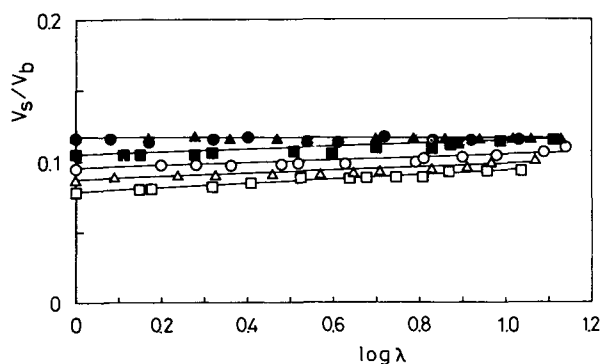


Fig. 15. Changes in the volume fraction of the side region against draw ratios. The marks are the same as those utilized in Figure 1.

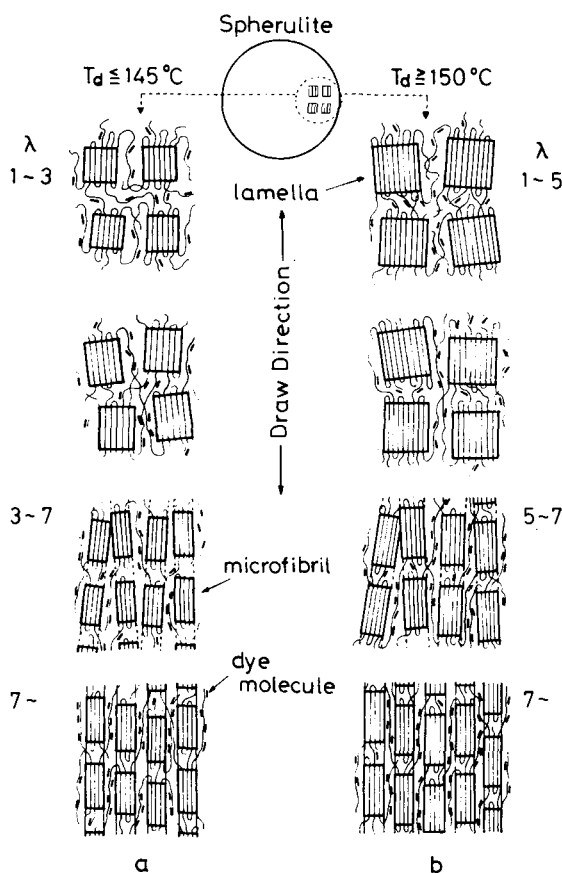


Fig. 16. Schematic models for change in dye sorption by PP films during drawing: (a) a model for PP films drawn below 145°C; (b) a model for PP films drawn above 150°C.

fiber axis in the lower range of  $\lambda$ , the channels for dye diffusion are bent and distorted, and they are not connected each other. The tortuosity of these channels decrease during drawing (the samples drawn above  $\lambda = 7$  in Fig. 16), and these channels are gradually oriented along the microfibrils. Therefore, the amount of sorbed Y-7 molecules in the side region becomes larger than that in the end region accompanied by drawing.

It is concluded that the mosaic block dyeing model for drawn polymers is available to interpret the complicated dye sorption behaviors of drawn PP films without introducing any void concepts. The dyeability in the side region is very important, and it governs the total dye sorption of the oriented polymers.

### References

1. H. Morizane, Y. Suda, and T. Shirota, *Sen-i Gakkaishi*, **27**, 113 (1971); *Chem. Abstr.*, **76**, 4794d (1972).
2. M. Sumida, N. Kusakabe, K. Miyasaka, and K. Ishikawa, *Nippon Kagaku Kaishi*, **1972**, 1165; *Chem. Abstr.*, **77**, 127317d (1972).
3. Y. Miyazawa, unpublished results.
4. F. J. Balta-Calleja and A. Peterlin, *Makromol. Chem.*, **141**, 91 (1971).

5. T. Masuko, S. Hasegawa, K. Yonetake, and M. Karasawa, *Makromol. Chem.*, **182**, 2049 (1981).
6. K. Yonetake, T. Masuko, T. Shimanuki, and M. Karasawa, *J. Appl. Polym. Sci.*, **28**, 3049 (1983).
7. K. Yonetake, T. Masuko, K. Takahashi, and M. Karasawa, *Sen-i Gakkaishi*, **40**, 294, (1984); *Chem. Abstr.*, **101**, 55894d (1984).
8. A. Weidinger and P. H. Hermans, *Makromol. Chem.*, **50**, 98 (1961).
9. F. Dannuso, G. Moraglio, and G. Natta, *Ind. Plast. Mod.*, **10**, 40 (1958).
10. H. P. Klug and L. E. Alexander, *X-ray Diffraction Procedures*, 2nd ed., Wiley, New York, 1974, Chap. 9, p. 656.
11. K. Nakayama, S. Okajima, and Y. Kobayashi, *J. Appl. Polym. Sci.*, **15**, 1453 (1971).
12. T. Masuko, M. Karasawa, K. Yonetake, and S. Okajima, *Sen-i Gakkaishi*, **32**, 496 (1976); *Chem. Abstr.*, **86**, 30400 (1977).
13. R. J. Samuels, *J. Polym. Sci., Part A-2*, **6**, 1101 (1968).
14. F. J. Baltá-Calleja and A. Peterlin, *J. Polym. Sci., Part A-2*, **7**, 1275 (1969).
15. F. J. Baltá-Calleja and A. Peterlin, *J. Mater. Sci.*, **4**, 722 (1969); F. J. Baltá-Calleja and A. Peterlin, *J. Macromol. Sci. Phys.*, **B4**(3), 519 (1970).
16. R. Hosemann, W. Wilke, and F. J. Baltá Calleja, *Acta Crystallogr., Sect. A*, **21**, 118 (1966).
17. A. Peterlin, *J. Polym. Sci.*, **C9**, 61 (1965).

Received October 24, 1984

Accepted January 28, 1985